



Nanoparticles for water desalination in solar heat exchanger

Mohadeseh Seyednezhad¹ · M. Sheikholeslami^{2,3} · Jagar A. Ali^{4,5} · Ahmad Shafee^{6,7} · Truong Khang Nguyen^{6,7}

Received: 10 March 2019 / Accepted: 24 July 2019 / Published online: 10 August 2019
© Akadémiai Kiadó, Budapest, Hungary 2019

Abstract

Producing potable water is a critical issue due to the lack of access to clean H₂O and the increasing demands of environment. One of the main technologies for water purification is solar still using the sustainable and green source of energy. To augment the efficiency of solar unit, nanoparticles are combined with the saline water. Nanofluids are suspended materials that besides the different geometries (single slope, double slope, tubular...) of the solar stills have a significant impact on improvement of the thermal conductivity of the brackish H₂O. Further, combining nanomaterial with solar energy system appears to be more cost-effective approach for potable water production since they boost the evaporation and condensation rate. This paper is a comprehensive literature on different types of nanofluid and various numerical, experimental and analytical methods that researchers have applied to augment the efficiency of system.

Keywords Nanofluid · Heat transfer · Desalination · Solar still · Evaporation · Condensation

List of symbols

A	Area
A_s	Area of the solar still in m ²
A_b	Area of the basin
F	Fluid
FESEM	Field Emission Scanning Electron Microscope
EPF	Energy production factor
H	Heat transfer coefficient
EPBT	Energy payback time

I_s	Current density of the surface
n	Number
ρ	Density
PCM	Phase change material
T	Temperature (°C)
UV	Ultraviolet
XRD	X-ray diffraction
η	Efficiency
\emptyset	Concentration of solid particles
W	West

✉ Ahmad Shafee
babac99@hotmail.com; ahmad.shafee@tdtu.edu.vn

¹ Department of Mechanical and Aerospace Engineering, Florida Institute of Technology, Melbourne, FL 32901, USA

² Department of Mechanical Engineering, Babol Noshirvani University of Technology, Babol, Iran

³ Renewable Energy Systems and Nanofluid Applications in Heat Transfer Laboratory, Babol Noshirvani University of Technology, Babol, Iran

⁴ Department of Petroleum Engineering, Faculty of Engineering, Soran University, Soran, Kurdistan Region, Iraq

⁵ Department of Petroleum Engineering, College of Engineering, Knowledge University, Arbil, Kurdistan Region, Iraq

⁶ Division of Computational Physics, Institute for Computational Science, Ton Duc Thang University, Ho Chi Minh City, Vietnam

⁷ Faculty of Electrical and Electronics Engineering, Ton Duc Thang University, Ho Chi Minh City, Vietnam

Subscripts

a	Ambient
ann	Annual
b	Basin surface
e	Evaporative
ebf	Evaporative base fluid
eff	Effective
en	Energy
ex	Exergy
giW	Inner condensing of the west side
giE	Inner condensing of the east side
in	Input

Introduction

Clean water is strong demand in environment that can save the life of human beings on the earth. The clean water is used for different purposes such as drinking, sanitation and

industrial application [1, 2]. Nanoscale materials have received an attractive application over different research fields particularly the clean and sustainable energy system such as fuel cells, solar cells and batteries, because of their capability to augment the yield and efficiency of the traditional devices [3–8]. A well-known example is using the nano-sized particles spread into the conventional fluid to enhance its thermal conductivity in heat transfer systems [9]. In this case, the liquid-containing suspended nanoparticles are called nanofluid, where the particles are in atomic size less than 100 nm [10–13].

Regarding that, nanotechnology-based heat transfer has changed our vision toward solar system by using nanofluids especially in solar stills (one type of desalination processes) due to the greater efficiency caused by the suspended nano-sized particles. The reason is they have a greater surface area, which decreases the thermal resistance of the brackish water and hence improves its thermal conductivity that favors water desalination process [12, 14, 15]. Therefore, nanofluids have been intensively used in forced convection of solar thermal systems as an ideal solution to improve the desalination process for potable and clean water [9, 16–18] due to their thermophysical properties them [8, 19].

World Health Organization reveals that about 663 million people around the world (particularly those living in rural areas) do not use improved potable water sources, due to unprotected springs and wells [16]. To obviate the needs of human, it is important to apply solar desalination system that has less pollution and make the water drinkable, even in remote areas. In that case, solar stills can provide freshwater with no greenhouse effects [20]. Since many decades ago, desalination technologies have improved enormously enabling almost all people worldwide to access the potable supply of water from brackish water (contains soluble salt) conversion [21].

Today, it is strongly important to combine desalination techniques using renewable energy resources the same as solar still, to prohibit the waste heat and to decelerate the global warming [22]. In general, it has been shown that desalination with solar still is superior over the conventional desalination processes due to the simpler installation and maintenance even in remote regions, cost-efficiency for customers and manufacturer and less air pollution due to fewer burning fuel in this process reducing the global warming effect [23, 24]. However, a comparison between conventional water desalination and the renewable one reveals that previously a quite larger area had to be allocated to such that technology in a power plants for water desalination, besides of having too many moving parts as heavy and high-pressure pump [25–27].

In previous years, several researches were done to study the various characteristics and elements that can improve

efficiency concerning the geographical situation as well as the weather condition of a typical region [28]. However, not only from the economic point of view, but also from the environmental aspect, nanofluids are among the first options that can boost the efficiency of solar collectors [29]. In current article, a review on variants techniques to improve the rate at which the fluid starts to evaporate and condense in different solar still geometries which using nanofluid has been discussed.

General mechanisms of thermal radiation and solar stills

The stem of a solar panel is its distillation processes that can produce freshwater in the large scale in that the brackish water starts vaporizing as solar radiation influences the black surface [30] of the collector and transferring the heat to the water on its surface increasing the water temperature. Then, the vaporized water will move upward and will occupy the whole container. As they reach the glass cover, they will turn into a cooled water droplet. This cooled air can be mixed with vapor droplets and carry them (convection process) for molecular precipitation through condensation process pouring them into the trough [31–35].

Nanomaterial in solar stills

There are main differences among various types of solar stills concerning the geometries and building materials, however, they all have three particular components; evaporator (convert salty liquid into pure liquid droplets), condenser (convert vapor droplets into liquid) and solar thermal collector (collect electromagnetic solar radiation) [36, 37]. Many researchers have investigated different techniques to improve the productivity such as adding extra condenser, ventilation and changing the geometry of the stills as well as using nanoparticles to obtain high evaporation rate [37]. It has been seen that surface temperature of the saline H_2O is greater using metallic nanoparticles in a fluid rather than non-metallic nanoparticle fluid [38] because of the thermal conductivity of metallic nanomaterial which has correlation with the size of the metallic particles [39, 40].

Different factors can affect the size of the particles including the PH, concentration, temperature and viscosity of the nanofluid [41, 42]. In fact, nano-sized particles are more stable in the suspension fluid rather than the larger-scale particles owing to higher ratio of surface area to the volume [42, 43]. Many researchers studied various aspects of thermal characteristics of the nanofluids empirically and

via theoretical methods, and they found that metallic oxide nanoparticles are thermodynamically more stable and have strong ability of solar radiation absorption because of their metallic characteristic. Hence, all of these properties make them more practical for nanofluids in solar still by improving their productivity [44, 45]. The geometry of solar stills differ mostly due to the weather condition, however, active and passive solar stills are the main two groups. Passive solar stills are those that do not use any mechanical devices pumps valves and controllers for water circulation or forced convection [36].

Single slope

There are many investigations to augment the yield of the SS-solar still [46]. Among them, Rashidi et al. [47] had a numerical and mathematical model (volume of the fluid—VOF) to verify their experimental setup to evaluate the condensation and evaporation rate. Al_2O_3 nanomaterial with volume fraction of 5% (Eq. (1)) has been utilized for a SS-Solar still. The comparison between the conventional still without nanofluid and the still modified with nanofluid

show that as nanofluid fraction rises from about 0% to around 5%, the efficiency, thermal and viscous entropy generation, all increase by 25%, 25% and 95%, respectively. They used Ansys-Fluent to compare the simulation both modified and non-modified conditions.

$$\rho_{\text{eff}} = (1 - \varphi)\rho_f + \varphi\rho_p \quad (1)$$

Figure 1 shows that for different nanofluid concentration ($\varphi = 0, \varphi = 5\%$) how the viscous and thermal entropy have changed. In addition, owing to the high-temperature gradient, the maximum viscous and thermal entropy were on those surface domains.

Other researchers, Gnanadason et al. [48] modified the system into a vacuum SS-Solar still investigated the impact of nanofluid on evaporation and condensation rate. However, to escalate the evaporation rate, they reduced the vapor pressure through the solar still chamber using a vacuum pump (it uses the atmospheric gravity and pressure and sometime by photovoltaic system) [27, 49, 50]. Alternatively, at low temperature the latent heat of condensation was used as a heat source for evaporation. Carbon nanotube (CNT: prepared by chemical vapor deposition—CVD) was synthesized in the laboratory and

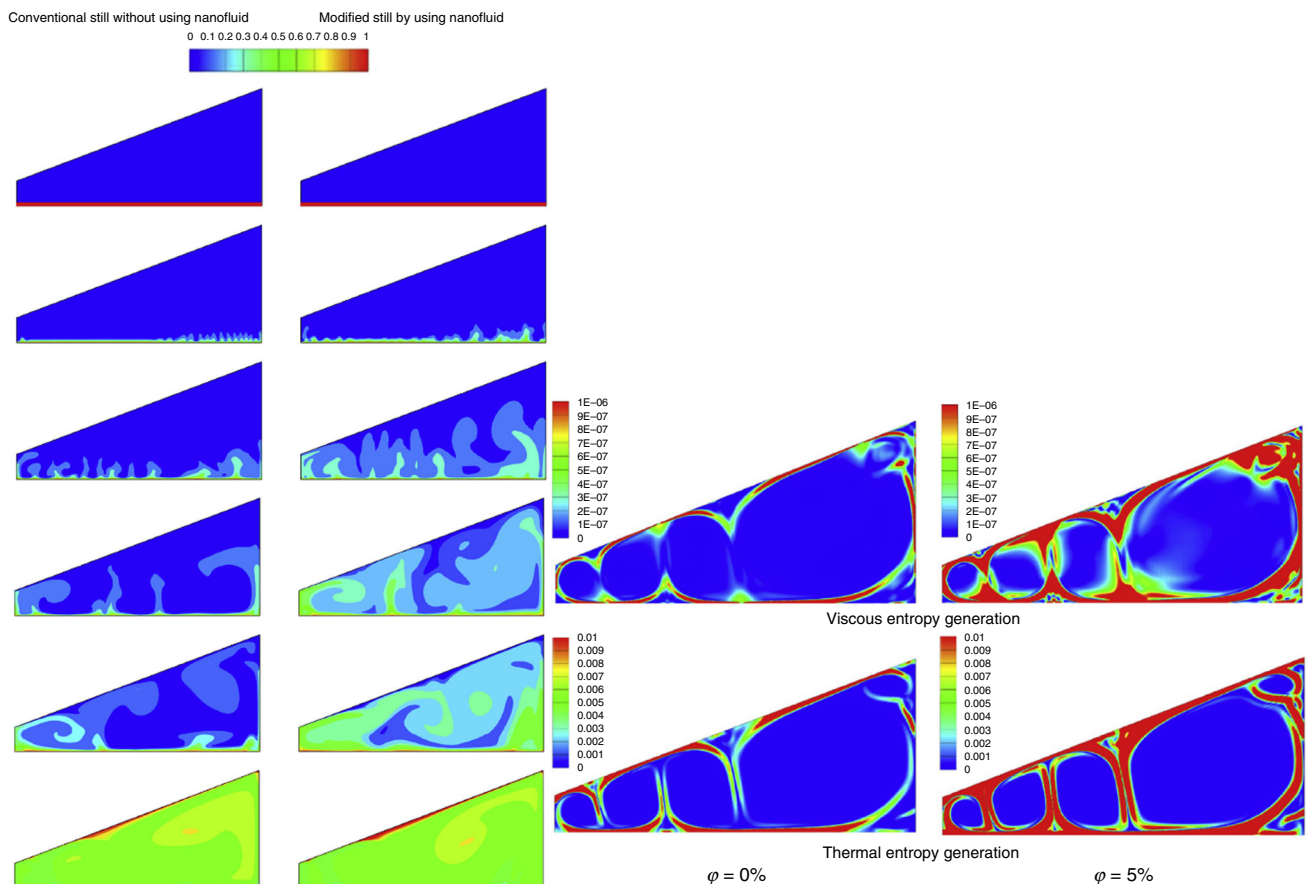


Fig. 1 (Left) vapor fraction for both systems at $\varphi = 5\%$ as time changes, (right) effect of nanofluid fraction on viscous and thermal entropy generation [47]

combined with brine water as nanofluid and then sodium dodecyl sulfate (SDS) surfactant (which has the ability to augment of water temperature) was used to make them stable in water. Figure 2 illustrates the improved productivity of the entire unit. In addition, to increase the evaporation rate (even at low temperatures) they reduced the pressure of the container that can release the latent heat during condensation process as well. With both vacuum pump and nanofluid, the efficiency increased by more than 40%.

Other metallic nanomaterials were used to develop the efficiency of the solar still. Sain and Kumawat [51] used Al₂O₃ nanoparticles (50–100 nm) combined with black paint of basin to have a rise in overall efficiency of the

system. They gained 12.18% higher thermal efficiency and 38.09% improvement in pure water production rate with using nanofluid. Table 1 demonstrates that the quality of the H₂O improved as the parts per million (PPM) of the raw H₂O increased due to using the nanofluid and black basin.

Kabeel et al. [52] reported productivity enhancement for the smaller size particles nanofluid (average size of 10–14 nm). As exhibited in Fig. 3, they have used numerical analysis to verify their experimental results to investigate the effect of a 0.025 and 0.3% Al₂O₃ and Cu₂O on a solar still with external condenser. In their experiments, the nanoparticles Al₂O₃ and Cu₂O had thermal conductivity of 46 and 76.5 W m⁻¹ K⁻¹, respectively.

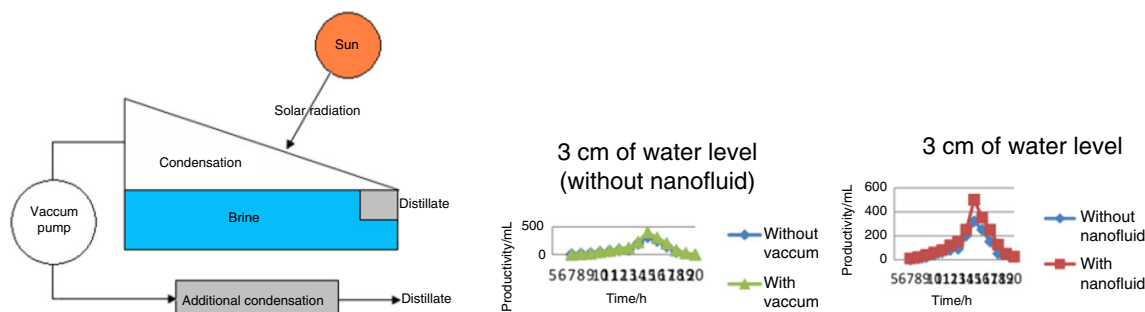


Fig. 2 The modified solar still with vacuum pump [48]

Table 1 The improved efficiency of the Al₂O₃ nanoparticles in single slope solar still at different water depth [51]

S. No.	Study parameter	Total quantity of the raw water/kg	TDS of sample water/PPM	Total collected water/kg	TDS of collected water/kg	Efficiency/%
1	Depth = 0.01 m	10	463	2.52	14	26.47
2	Depth = 0.02 m	20	496	2.4	16	31.62
3	Depth = 0.03 m	30	520	2.36	15	38.16
4	Depth = 0.01 m, nanoparticles used	10	414	3.48	14	38.65

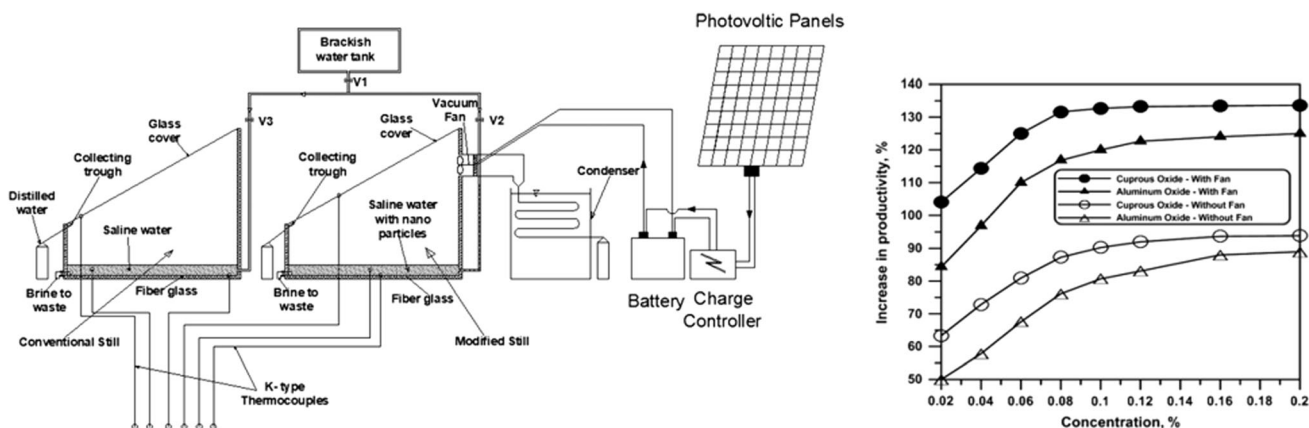


Fig. 3 (Left) schematic of the solar still using nanofluid and vacuum, (right) the productivity result of the system with fan and without fan [55]

They reported that evaporation and condensation ratio and the heat transfer coefficient of cuprous oxide in the new shape of solar still are higher than the non-modified one. They also verified that the daily performance of a nanofluid with Al_2O_3 is higher than Cu_2O nanoparticles in the water in both of the conventional and modified [52–54].

Hence in order to improve the system using Cu_2O as the nanofluid, Kabeel et al. [55] applied a vacuum fan to the conventional solar still. They took the best concentration of the nanofluid by using X-ray diffraction technique. Results showed that the metallic nanoparticle of Cu_2O with the presence of fan augments the productivity of the still unit thanks to the higher thermal conductivity of the cuprous oxide than aluminum oxide.

To augment the effectiveness of the nanofluid, Thakur et al. [56] used the black paint basin to boost the absorptivity ratio of the solar still. In addition, to augment the evaporation rate the nanoparticles of Al_2O_3 were added to the brine water. They revealed that the efficiency per 12 h (starting at 7:00 p.m.) increased to about 47.575 and

44.14% with the presence of the nanopaint and nanofluid, respectively.

Another approach to enhance the yield and productivity is using the PCM that can augment the thermal conductivity of the solar still because of its capability to store the latent heat of the material in large quantities [50, 57]. In this way, Rajasekhar and Eswaramoorthy [58] used the Al_2O_3 dissolved in paraffin wax (phase change material) in which it has the ability to store the latent heat of the fluid (Fig. 4). Furthermore, they compared the thermal productivity of the solar still in different conditions; using nanoparticles spread in paraffin, merely paraffin and with no paraffin. In their studies, the PCM material has the daily efficiency of about 45%, which was higher compared to 40% and 38% of solely paraffin wax and no paraffin, respectively. In Eq. (2), m is the mass of PMC (kg) in saline water per hour, L is the latent heat, S is the glass surface area (m), and I is the irradiation of solar energy ($W m^{-2}$).

Fig. 4 (Left) schematic of the experimental setup of the PCM material in basin water, (right) daily efficiency of the three different experimental setup [58]

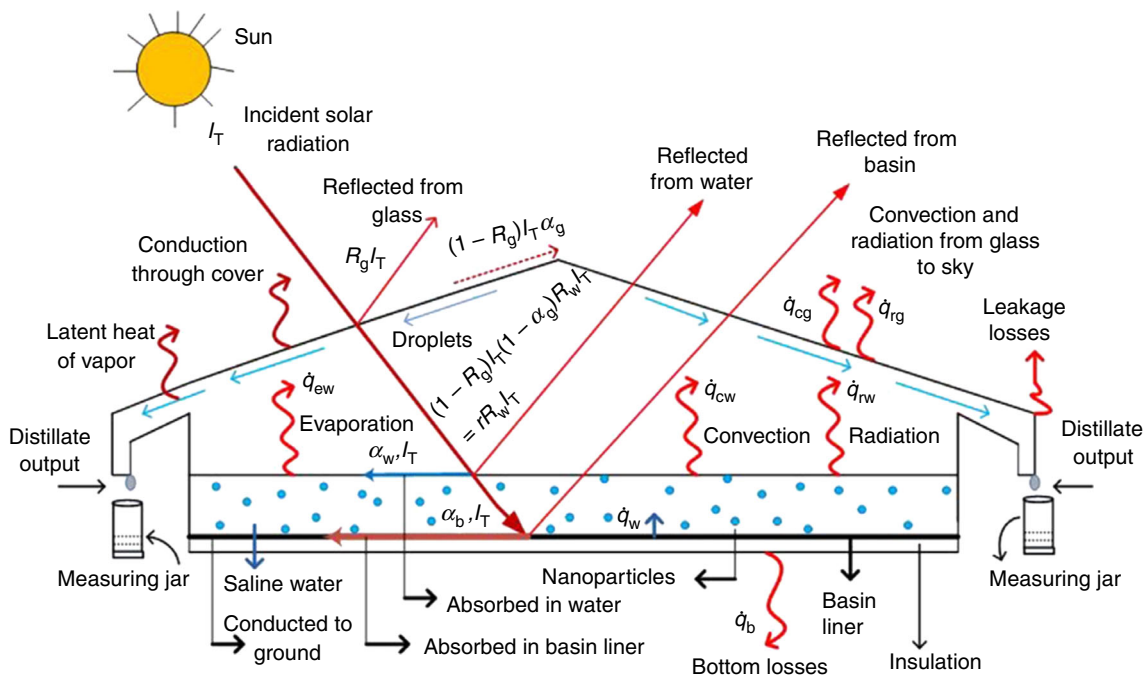
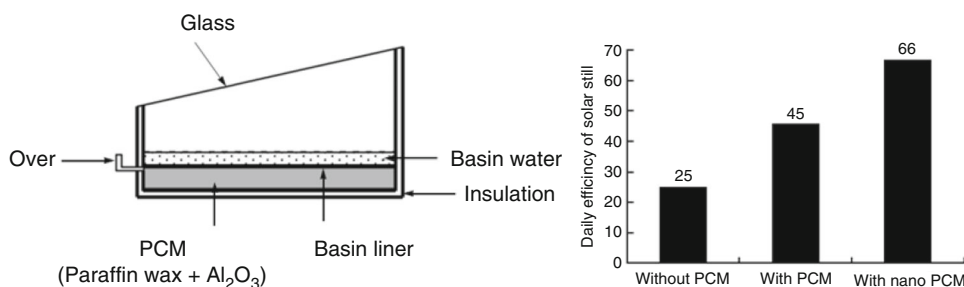


Fig. 5 The schematic of a double slope solar still with nanoparticles [45]

$$\eta_{\text{daily}} = \frac{\sum mL}{S \sum I} \tag{2}$$

Double slope/cascade

Double slope solar still can operate at higher temperature rather than the SS-Solar stills [59, 60]. Different nanofluids are used to have an augmentation in the performance of the solar desalination unit. Sahota et al. [45, 61] revealed that the thermal energy (Eq. (3)) of 50.34% of alumina nanomaterial in the base fluid, and 46.10% of TiO₂ and 43.81% of copper oxide nanomaterial in a passive double slope solar still was greater than the conventional solar still (Fig. 5). The thermal conductivity of those concentrations are 38.5, 11.8 and 17.6 W m⁻¹ K⁻¹ for Al₂O₃, TiO₂ and CuO, respectively. Using a thermal modeling, they found that 35 kg Al₂O₃ nanofluid could make a higher temperature difference (ΔT) between the; hence more evaporation happens (Fig. 6).

$$\eta_{\text{hourly,ex}} = \left(\frac{1}{0.933 \times A_s \times I_s(t)} \right) \left\{ h_{\text{ebf,E}} \left[(T_{\text{bf}} - T_{\text{giE}}) - (T_a - 273) \ln \left(\frac{T_{\text{bf}} + 273}{T_{\text{biE}} + 273} \right) \right] + h_{\text{ebf,W}} \left[(T_{\text{bf}} - T_{\text{giW}}) - (T_a + 273) \ln \left(\frac{T_{\text{bf}} + 273}{T_E + 273} \right) \right] \right\} A_b \tag{3}$$

From experimental result on passive double slope solar still, Sahota and Tiwari [62] reported the improved efficiency using Al₂O₃ nanoparticles with 0.04%, 0.08% and 0.12% concentrations suspended into 35 and 80 kg water. The reason for choosing Al₂O₃ among ZnO, Fe₂O and SnO, was its better productivity for passive solar stills. As a result, the daily yield improved by increasing the concentration of Al₂O₃ (Fig. 7) and the solar still yield enhanced for 8.4% and 12.2% for 80 and 35 kg base fluid correspondingly (Fig. 8). The point is the nanoparticle in the

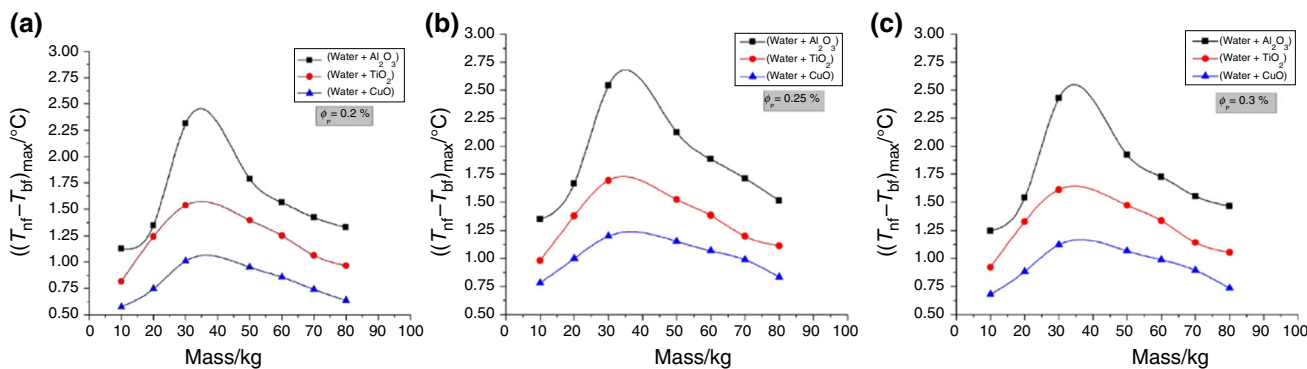


Fig. 6 Plots for maximum temperature variation (ΔT)_{max} for three different nanofluids (Al₂O₃, TiO₂ and CuO nanoparticles dissolved in water) with three different mass concentrations: **a** 0.2%, **b** 0.25% and **c** 0.3% [45]

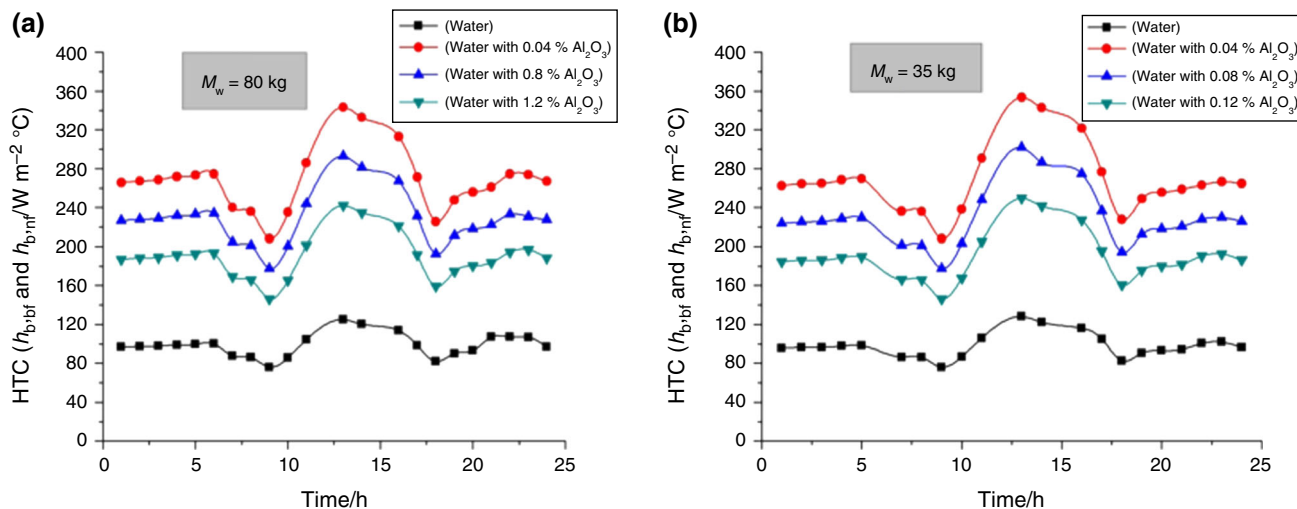


Fig. 7 The convective heat transfer coefficient for water and nanofluid for three different concentrations in 35 and 80 kg brine water [62]

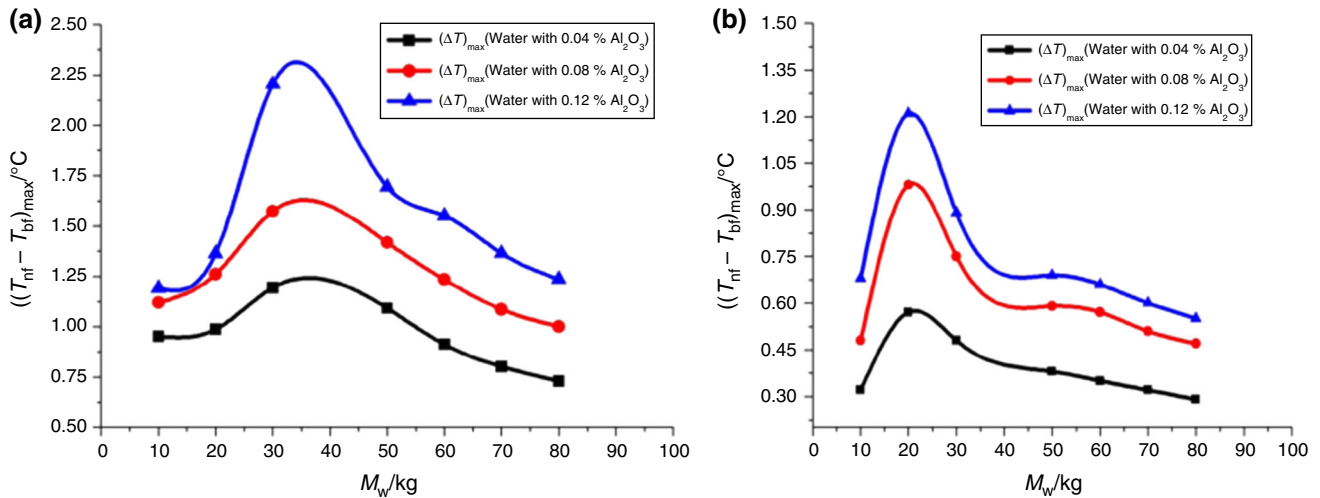


Fig. 8 The $(\Delta T)_{\max}$ between the nanofluid and water as based fluid [62]

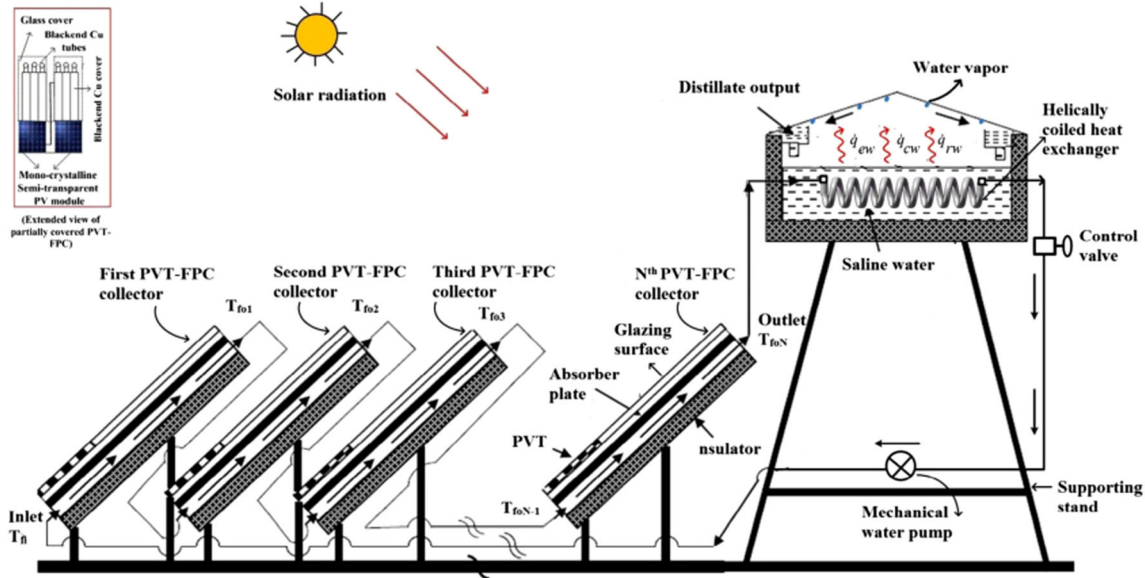


Fig. 9 The schematic of the Hybrid double slope solar still, without coil heat exchanger [64]

base fluid can directly absorb those radiation spectrums that are matched with their own optical spectrum.

In another experimental and numerical study [63–65] they analyzed the finalized cost for the two types of the nanofluids (CuO and Al₂O₃) for the active hybrid double slope solar with and without heat exchanger using helical coil as depicted in Fig. 9. It appears that using coil increased water temperature and that resulted in a greater temperature difference. In both cases, the EPBT (Eq. (4)), the EPF (Eq. (5)) and ICCE (Eq. (6)). They revealed that these three energy parameters are lead to better annual performance and environmental cost by using nanofluid, and helical coil heat exchanger and CuO nanofluid. The maximum LCCE over 50 years of life span reached to the

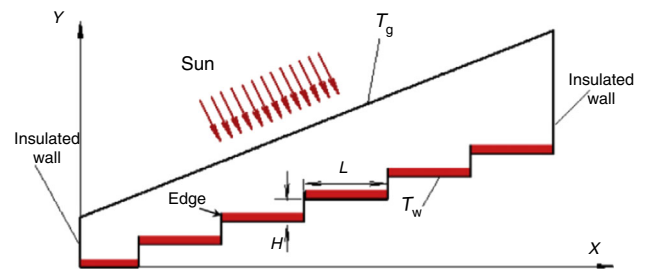


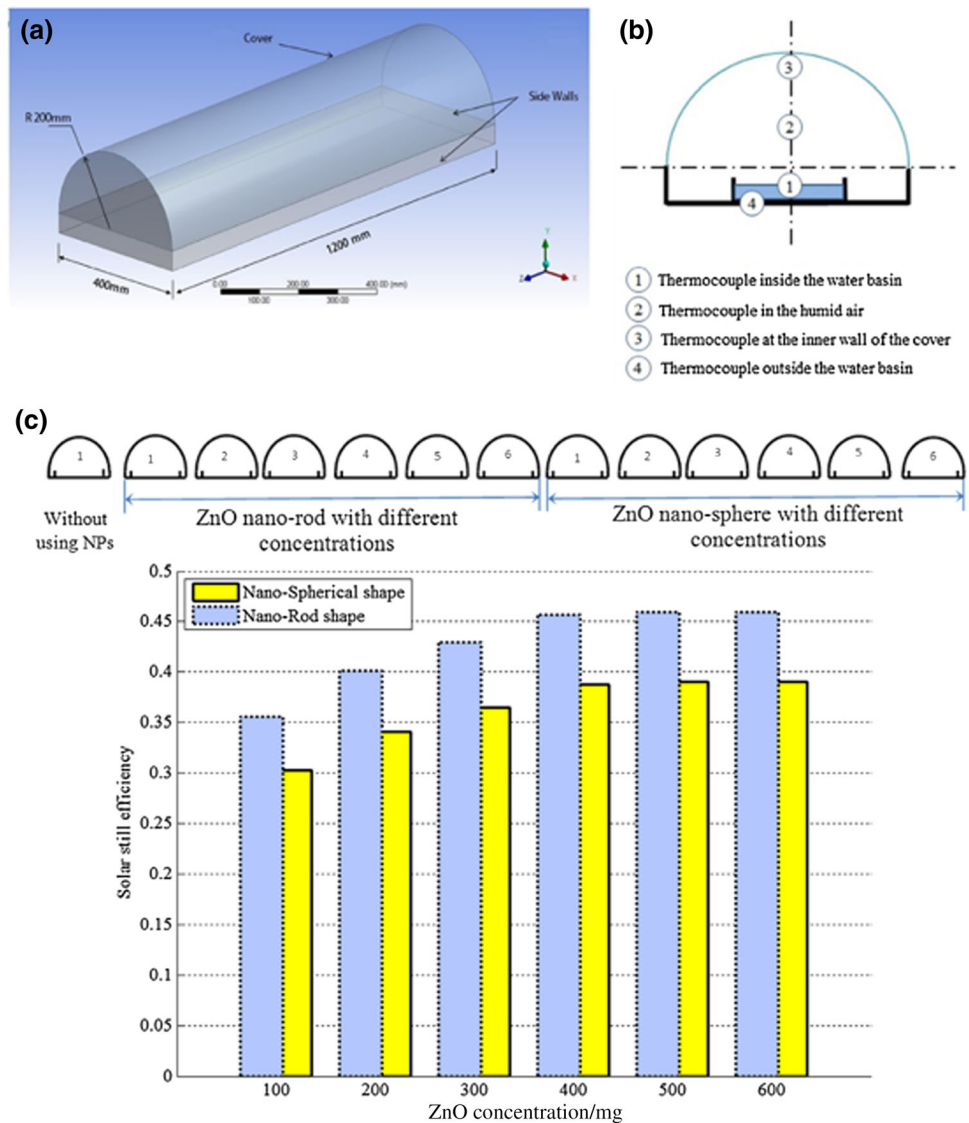
Fig. 10 The schematic of the cascade solar still with $T_g = 40\text{ }^\circ\text{C}$, $\text{Height}_{\text{left}} = 0.06\text{ m}$, $\text{Height}_{\text{right}} = 0.57\text{ m}$, $L = 0.57\text{ m}$ [66]

14.8% and 10.8% correspondingly for both systems using CuO nanofluid while it was 2.55 for the Al₂O₃ nanofluid in conventional system.

Table 2 The comparison between the RSM and CFD results for different Al₂O₃ concentration [82]

Solid volume fractions	Real optimized parameters		Hourly productivity predicted by RSM	Hourly productivity calculated by CFD	Error%
	H/cm	L/cm			
Φ = 0%	2.73	12.80	205.88	201.56	2.1
Φ = 1%	2.34	12.63	213.40	209.40	1.9
Φ = 2%	2.39	12.74	222.59	217.80	2.2
Φ = 3%	2.58	12.78	232.84	227.38	2.4
Φ = 4%	2.43	12.68	242.41	238.12	1.8
Φ = 5%	2.35	12.66	250.72	245.56	2.1

Fig. 11 (Top) schematic of the tubular solar still (a) with thermocouples (b), (bottom) effect of concentration on the efficiency of the half-tubular solar still [69]



$$EPBT_{en/ex} = \frac{E_{in}}{E_{out,ann}} \text{ years}$$

$$(4) \quad EPF_{en/ex} = \left[\frac{E_{in}}{E_{out,ann}} \right]^{-1} \tag{5}$$

$$LCCE_{en/ex} = \frac{(E_{en/ex,ann} \times n) - E_{in}}{E_{sol,ann} \times n} \tag{6}$$

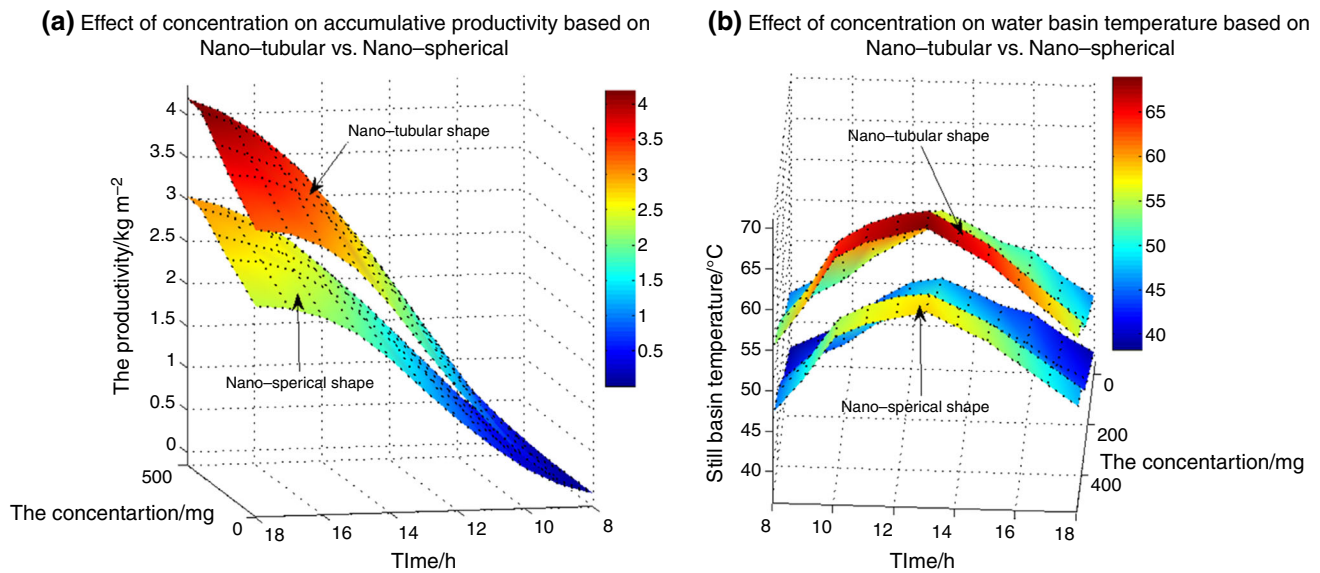


Fig. 12 The comparison between effect of the two morphology and concentration of the nanoparticles on the productivity and water temperature [69]

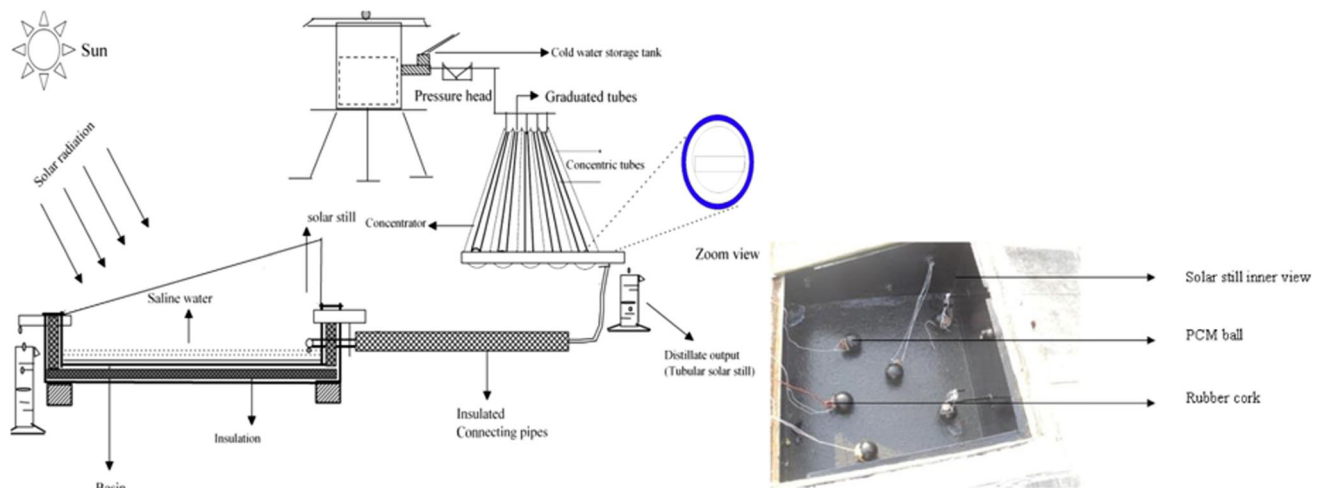


Fig. 13 The schematic of the modified system which is the combination of the concentric tubular solar still and the parabolic concentrator [81]

In this regard, Rashidi et al. [66] demonstrated the impact of nanofluid on cascade solar still (Fig. 10) by decreasing the space between the glass and the surface of the collector and the time for transferring water vapor into condenser surface [67]. The CFD results show that there will be a 22% improvement in hourly productivity by augmenting the concentration of Al_2O_3 from 0 to 5%. The response surface methodology (RSM) proves that the effect of step's height is more than step's length on productivity (Table 2).

Tubular

Another type of passive solar still is tubular solar still which mostly used in humid weather condition [68, 69]. The effect of the solvent on nanofluid properties was found by Saleh et al. [70] using a different synthesis method such as FESEM, TEM, UV-vis spectroscopy and XRD, for ZnO nanomaterials. In their research, were added to the black paint basin with wide concentration range from 0 to 600 mg of each 0.001 L of the black paint. They revealed that the rod-shaped ZnO nanoparticles improved the

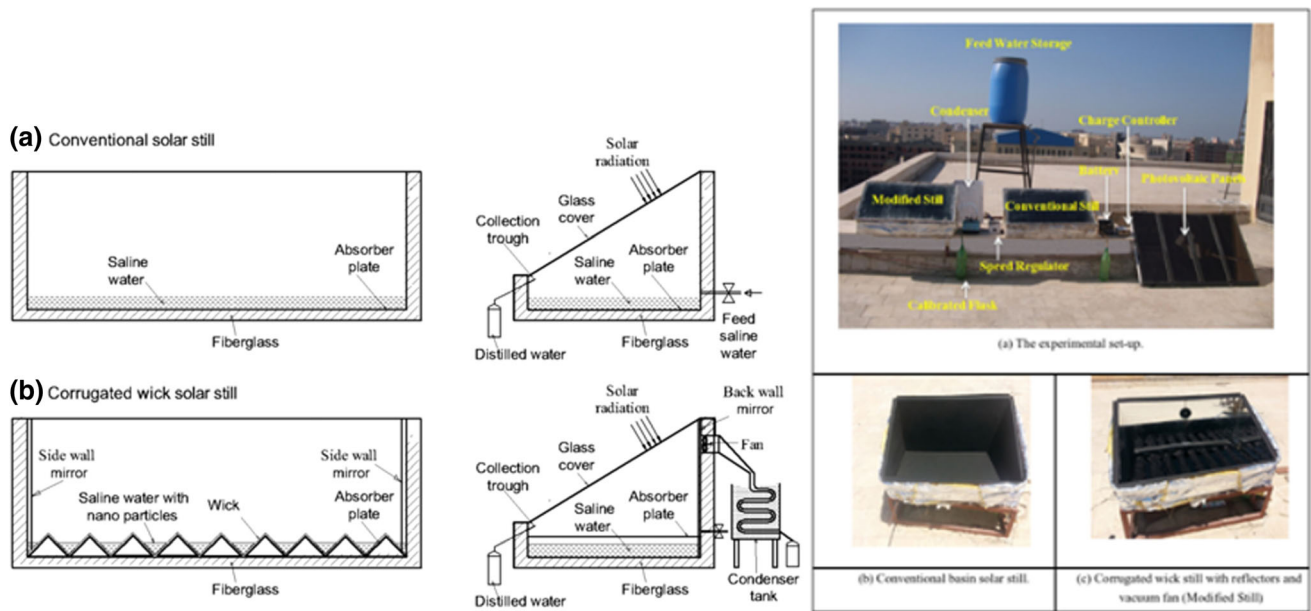


Fig. 14 The schematic of the experimental setup of the corrugated wick solar still with vacuum and mirrors [71]

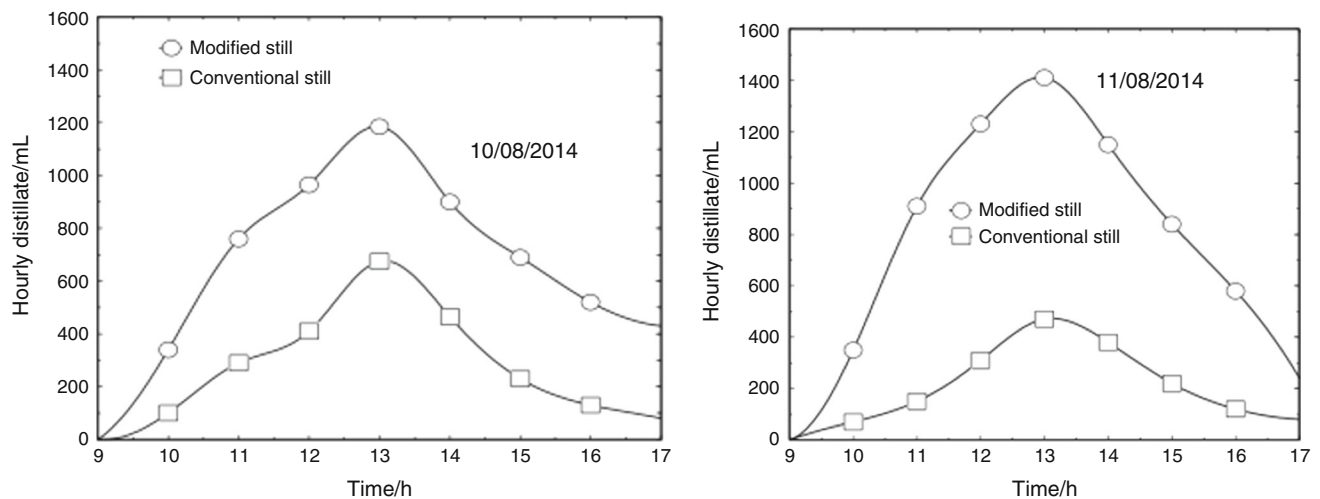


Fig. 15 The daily distillate rate for the grooved wick solar still with vacuum and mirrors and Cu_2O nanofluid [71]

efficiency of the solar still to 30% and 38%, respectively, compared with nanospherical-shaped particles (Figs. 11 and 12).

The reason is the rod-shaped ones have more surface area and less rough edge and face, which made them to be homogeneously distributed in fluid.

However, Arunkumar et al. [71, 72] found another way to have productivity growth of the nanofluid tubular solar still (TSS). They combined a parabolic concentrator with a tubular solar still with specific thermodynamic properties as $(\frac{1}{\sin(\theta a)})$, where θa is a half-angle of the solar incident on the receiver. Hence, this characteristic can raise the temperature besides using paraffin wax and PCM to increase

the evaporation rate as they discharge the stored latent heat of the brine water [57]. Combination of PCM and the brine water can increase the evaporation rate at night (Fig. 13). They showed that heat transfer coefficient improved to about 700% and 176% for the TSS and the concentric-TSS, both with the compound parabolic concentrator, respectively, compared to the non-modified TSS which was about $50 \text{ W m}^{-2} \text{ K}^{-1}$.

Other types of solar still

There exist some solar still designs that cannot be categorized in any of the aforementioned groups. For example, Omra et al. [73, 74] conducted three case experiments for a

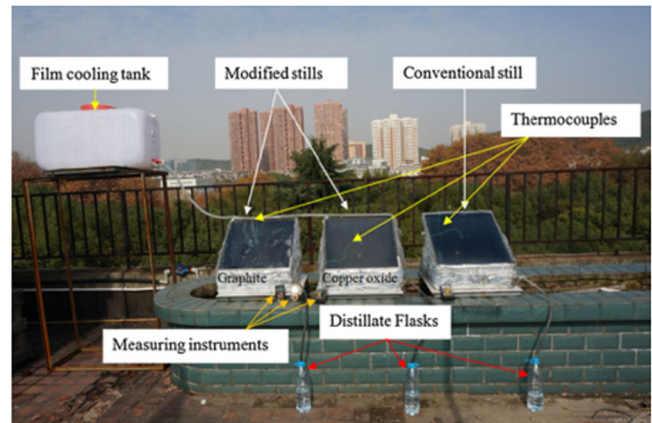
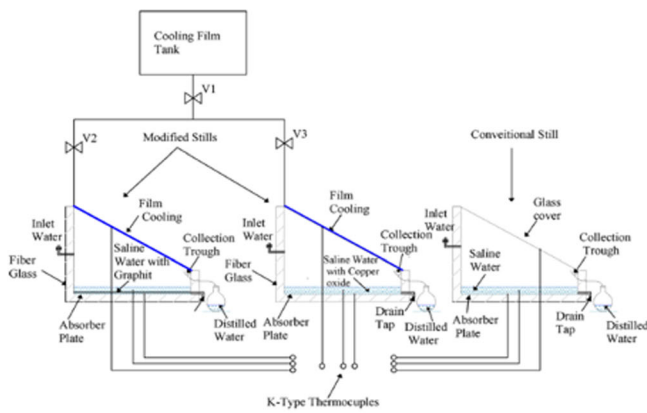


Fig. 16 The experimental setup for solar still with glass shield cooling [73]

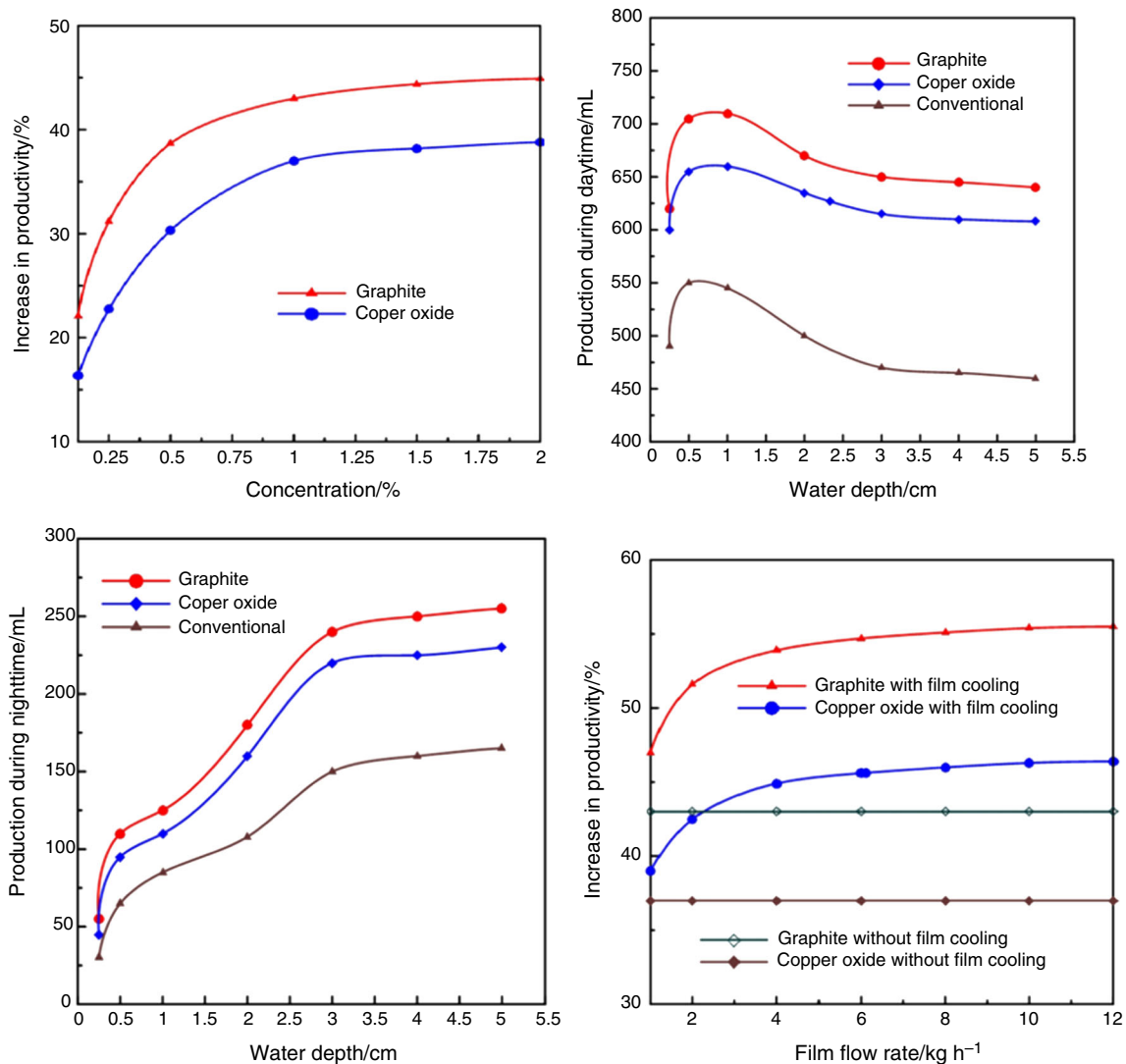


Fig. 17 Increase in productivity for solar still with glass cover cooling with different nanofluid concentrations and different base fluid depth for daytime and nighttime, and effect of flow rate on productivity [73]

Fig. 18 Experimental setup for the modified solar still with the same initial condition using a same brine water tank [76]

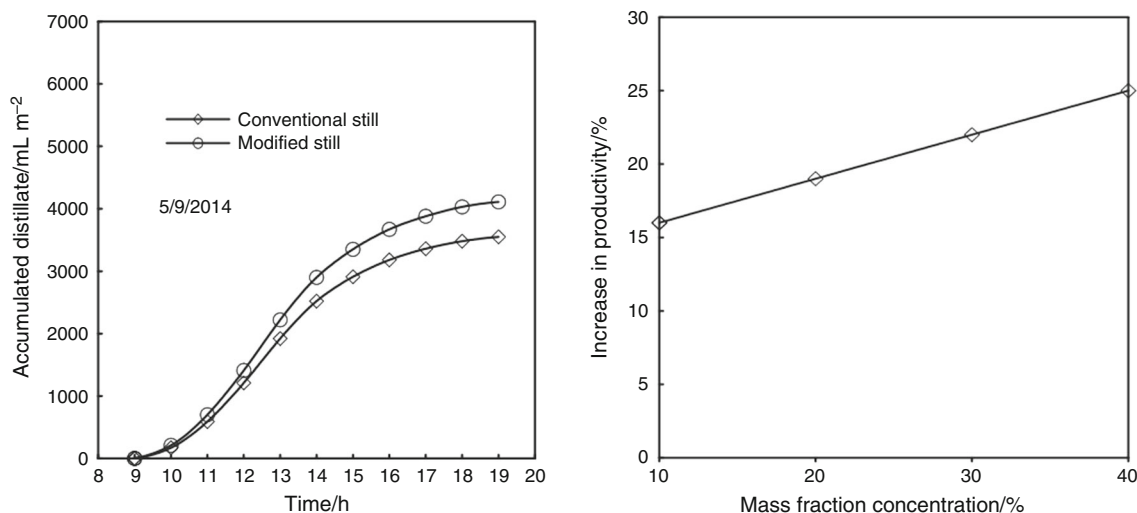
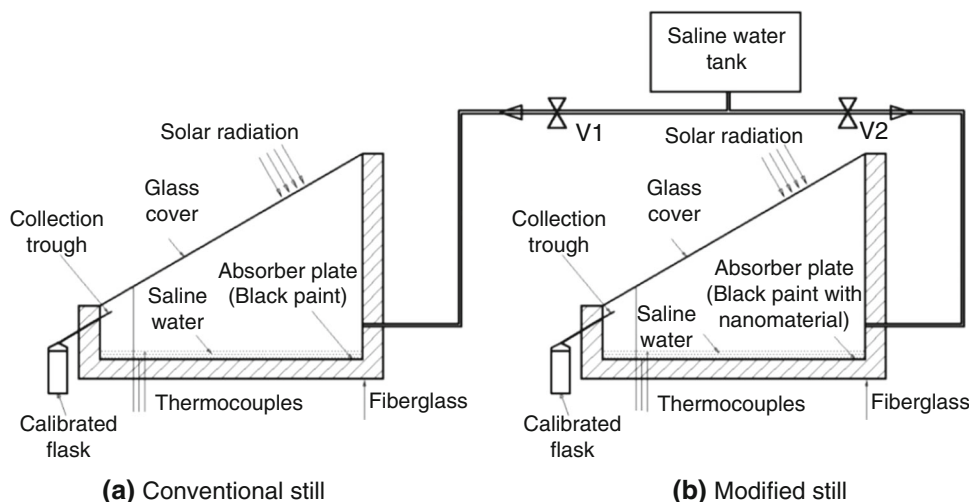


Fig. 19 Improved productivity of the black-coated basin with CuO nanofluid [76]

simple corrugated wick solar still equipped with a vacuum fan and then wall mirrors [72]. They reported that the hourly distillate water was higher compared to the conventional solar stills since the enhancement in the condensation and evaporation rate was due to different factors including the nanofluids (Cu₂O and Al₂O₃ with water), vacuum fan, V-shape wick and mirrors (Fig. 14). In which the productivity of system with vacuum and mirror was higher than with vacuum only as illustrated in Fig. 15.

Another group also proved that using CuO in active solar stills appears to be more effective than the Al₂O₃ nanofluid in conventional stills. Sharshir et al. [75, 76] demonstrated that the combination of single slope solar stills can lead to a new modified design that enhances the effect of CuO (Fig. 16). They operated an experiment with various water depth and different cooling rate using

different concentrations of CuO micro-flakes and graphite with thermal conductivity of 76 and 129 W m⁻¹ K⁻¹ and the average particle size of less than 2 μm. They found the ideal nanofluid concentration for 1% and the optimum 0.5 and 1 cm water depth for CuO micro-flakes and graphite, respectively. The maximum productivity was 53.95% with glass cooling and 43.10% without glass cooling for 1% CuO nanofluid with 0.5 depths of the brackish H₂O. The daily efficiency of unit with cooling flow over the glass increased by 46% and 49% for CuO and graphite correspondingly (Fig. 17).

However, Fig. 17 shows that in all cases graphite has higher productivity during both daytime and nighttime and that endorses the superiority of graphite over CuO for the combined design. Because the graphite particles have lower density than copper (II) oxide particles and this

Table 3 Summary of the type of nanoparticles, geometry of the solar still and the location of the experiment

References No.	Geometry	Technique used	Location	Nanoparticles
[45]	Passive double slope solar still	Thermal modeling Experimental climate data	New Delhi, obtained from IMD Pune, India.	Al ₂ O ₃ , TiO ₂ , CuO
[53]	Single basin solar still with external condenser	Experimental	Kafrelsheikh city, Egypt	Al ₂ O ₃
[71]	Corrugated wick solar still with reflectors	Experimental	Kafrelsheikh city, Egypt	Al ₂ O ₃
[55]	Solar still with vacuum	Experimental	Kafrelsheikh city, Egypt	Al ₂ O ₃ , CuO
[52]	Stepped solar still	Numerical	Kafrelsheikh city, Egypt	Al ₂ O ₃ , CuO
[48]	Single basin solar still	Experimental	Valsad, Gujarat, India	Al ₂ O ₃
[73]	Solar still	Experimental	Wuhan, China (Latitude 29_58_N and longitude 113_53_E)	CuO graphite micro-flakes
[66]	Cascade solar still	Optimization	Iran	
[56]	Passive single basin solar still	Comparative study numerical	Jaipur, India	Al ₂ O ₃
[83]	Single slope solar still	Numerical		Al ₂ O ₃
[51]	Single slope solar still	Experimental	Jabalpur, India	CuO
[84]	Passive solar still	Experimental	–	Al ₂ O ₃ , TiO ₂ , CuO
[7]	Hybrid double slope solar still	Experimental	New Delhi (India)	CuO
[61]	Passive double slope solar still	Experimental	New Delhi (India)	Al ₂ O ₃ , TiO ₂ , CuO
[85]	Passive double slope solar still	Experimental	New Delhi (India)	Al ₂ O ₃ , TiO ₂ , CuO
[86]	Conventional double slope solar still	Experimental	Gujarat, India	Al ₂ O ₃
[87]	Solar still	Experimental	China	SiC
[69]	Solar still (basin type)	Experimental	Egypt	ZnO
[88]	Passive solar still	Experimental	Jabalpur, India	CuO
[89]	Solar still	Experimental	Southern Algeria	–
[90]	Solar still	Theory	Gujarat, India	–
[76]	Pyramid solar still	Experimental	India	CuO
[58]	Solar still	Experimental	India	Al ₂ O ₃
[91]	Tubular solar still	Experimental	India	PCM

makes them to have homogenous distribution in the base fluid [74].

As it is mentioned, CuO nanofluid has often used in the forced convection systems. Gupta et al. [77] augmented the thermal conductivity of the passive solar still by using the CuO nanoparticles to escalate the heat transfer surface area which enhances the productivity of the modified system to 22.4% higher than the conventional one and that endorses a

better yield. Their results were confirmed by Kabeel et al. [78] who used the same nanoparticles (CuO) mixed with black paint for the inside surface of the basin to increase the thermal conductivity. In their system, they used a tank to have the same initial conditions for both conventional and modified still (Fig. 18). It is proved that there is an increase in their modified system using nanofluid and the

Table 4 Cost per liter per day for different types of solar still in USA [78]

Types of still	References No.	System unit cost in US \$	Daily yield output	Per liter water cost for 1 year (let 300 sunny days in a year) payback period in US \$
Single slope	[40, 48]	79.95	4.1 l ⁻¹ m ⁻² day ⁻¹	0.065
		100	1.7 l ⁻¹ m ⁻² 0.54 day ⁻¹	0.196
Double slope hybrid	[19, 21, 50]	200	3.070 l ⁻¹ m ⁻² day ⁻¹	0.217
		879.56	7.54 l ⁻¹ m ⁻² day ⁻¹	0.388
		550	12.48 l ⁻¹ m ⁻² day ⁻¹	0.027
Hemispherical	[25, 26]	233 m ⁻²	4.2 l ⁻¹ m ⁻² day ⁻¹	0.017
		958	5.7 l ⁻¹ m ⁻² day ⁻¹	0.560
Pyramidal miscellaneous domestic designs	[51–53]	582.3	4.1 l ⁻¹ m ⁻² day ⁻¹	0.065
		35.03	1.6 l ⁻¹ m ⁻² day ⁻¹	0.072
		290	1.2 l ⁻¹ m ⁻² day ⁻¹	0.805

Table 5 Thermal conductivity and cost of different quantities of nanoparticles for nanofluids [80]

SI. No.	Nanopowders	Thermal conductivity/W m ⁻¹ K ⁻¹	Quantity/g	Cost/Rs
1	Aluminum oxide (Al ₂ O ₃)	40	25	200
2	Zinc oxide (ZnO)	29	100	1500
3	Tin oxide (SnO ₂)	36	25	1500
4	Iron oxide (Fe ₂ O ₃)	7	25	1750
5	Gold nanopowders (Au)	315	1	35,029
6	Titanium dioxide (TiO ₂)	8.5	100	12,859
7	Copper oxide (CuO)	76	5	3111
8	Carbon nanotubes	3000–6000	250	19,521
9	Zirconium (IV) oxide (ZrO ₂)	2	100	10,611
10	Silicon nitride (Si ₃ N ₄)	29–30	25	11,434
11	Boron nitride (BN)	30–33	50	4911
12	Aluminum nitride (AlN)	140–180	50	5193
13	Diamond nanopowders (C)	900	1	8755
14	Silver nanopowders (Ag)	424	5	12,917

highest productivity was achieved at 40% concentration of the nanoparticles (Fig. 19).

Among all metallic nanoparticles, silicon carbide (SiC) is a semiconductor material that can boost the conduction mode of the brine water. Chen et al. [79] synthesized the SiC nanofluid uniformly in laboratory and then showed that it has a great effect on thermal conductivity and radiation absorption of the seawater. They found that as the salinity intensity, the stability level decreased. Besides the optical features of the nanomaterial, different salt concentration in seawater was examined to find the stable condition and the best thermal conductivity. The novelty of their experiment was using the UV–vis spectrometer and optical properties of the nanofluid to study the effect of salinity on nanofluid. They proved that metallic oxides have superior thermal conductivity and optical properties, and low luminousness improves the absorptivity for desalination. Besides the important achievements of the researchers, Table 3

demonstrates a comprehensive summary of the different types of nanofluid that researchers used for various locations and geometries of solar stills.

Cost evaluation

Usually using renewable energy as solar desalination devices appears to be costly but in the long period. Yadav et al. [89] showed that the payback of solar stills without using the nanofluid depends on manufacturing cost (fixed cost), and operating cost (variable cost) when the lifetime of the solar stills vary between 5 and 10 years for various kinds of solar stills (Table 4). Besides the other components of the solar still such as pumps, pipes, tank and control devices, using nanofluid will adds up to the capital cost [70, 79]. Elango et al. [91] provided a table for different nanoparticles that can be combined with saline

water. It appears that Al_2O_3 synthesizes has reasonable cost among the other types of nanopowders (Table 5). Several nanomaterials were utilized in recent years to augment thermal features [92–111].

Conclusions

From the literature, the density of the nanoparticles plays a significant role in the quality of their distribution. That means the lower density leads to higher concentrations of the nanopowders within pure fluid and this boosts the thermal conductivity of the nanofluids, particularly in laminar convection. The volume fraction, size and shape of the suspended nanoparticles are the other important factors that have a correlation with thermal conductivity in either flow patterns. In all cases, the volume fraction of the nanoparticles did not go beyond a limit to avoid making it into a non-Newtonian fluid. For the modified systems that used a fan to have a forced convection, an increase in convection coefficient leads to an augment temperature gradient. In other words, higher condensation rate was achieved due to improving the thermal conductivity of the brine H_2O . Furthermore, Al_2O_3 seemed to be the best choice in terms of the solar still with natural convection.

Suggestions for the future research

It appears that besides using nanofluids some of the researchers applied mechanical devices such as pressure and vacuum pump and fan, and using an extra condenser. However, this cycle needs some extra power and energy. It is suggested to install a photovoltaic (PV) panel on the ceiling of a building and the extra heat at the rear side of the PV panel can be used to increase the evaporation rate. Although this may not be a cost-effective approach, in long term it will have payback for users.

References

1. Nayi KH, Modi KV. Pyramid solar still: a comprehensive review. *Renew Sustain Energy Rev.* 2018;81:136–48.
2. Kaushal A, Varun. Solar stills: a review. *Renew Sustain Energy Rev.* 2010;14(1):446–53.
3. Huang Z-F, et al. Carbon nitride with simultaneous porous network and O-doping for efficient solar-energy-driven hydrogen evolution. *Nano Energy.* 2015;12(Supplement C):646–56.
4. Seyednezhad M, Rajabi A, Muchtar A, Somalu MR, Ooshak-saraei P. Effect of compaction pressure on the performance of a non-symmetrical NiO–SDC/SDC composite anode fabricated by conventional furnace. *J Asian Ceram Soc.* 2017;5(2):77–81.
5. Ni G, et al. Volumetric solar heating of nanofluids for direct vapor generation. *Nano Energy.* 2015;17(Supplement C):290–301.

6. Chen Y, et al. Low temperature solid oxide fuel cells with hierarchically porous cathode nano-network. *Nano Energy.* 2014;8(Supplement C):25–33.
7. Sahota L, Tiwari GN. Exergoeconomic and enviroeconomic analyses of hybrid double slope solar still loaded with nanofluids. *Energy Convers Manag.* 2017;148(Supplement C):413–30.
8. Saidur R, Leong KY, Mohammad HA. A review on applications and challenges of nanofluids. *Renew Sustain Energy Rev.* 2011;15(3):1646–68.
9. Abu-Nada E, Masoud Z, Oztop HF, Campo A. Effect of nanofluid variable properties on natural convection in enclosures. *Int J Therm Sci.* 2010;49(3):479–91.
10. Minkowycz W, Sparrow EM, Abraham JP. Nanoparticle heat transfer and fluid flow. Boca Raton: CRC Press; 2012.
11. Daungthongsuk W, Wongwises S. A critical review of convective heat transfer of nanofluids. *Renew Sustain Energy Rev.* 2007;11(5):797–817.
12. Godson L, Raja B, Lal DM, Wongwises S. Enhancement of heat transfer using nanofluids—an overview. *Renew Sustain Energy Rev.* 2010;14(2):629–41.
13. Hussein AM, Sharma KV, Bakar RA, Kadirgama K. A review of forced convection heat transfer enhancement and hydrodynamic characteristics of a nanofluid. *Renew Sustain Energy Rev.* 2014;29:734–43.
14. Colangelo G, Favale E, Miglietta P, de Risi A, Milanese M, Laforgia D. Experimental test of an innovative high concentration nanofluid solar collector. *Appl Energy.* 2015;154(Supplement C):874–81.
15. Elias Jamil, Bechelany Mikhael, Utke Ivo, Erni Rolf, Philippe Laetitia. Urchin-inspired zinc oxide as building blocks for nanostructured solar cells. *Nano Energy.* 2012;1(5):696–705.
16. Organization WH, Supply WUJW, Programme SM. Progress on sanitation and drinking water: 2015 update and MDG assessment. Geneva: World Health Organization; 2015.
17. Sheikholeslami M, Seyednezhad M. Lattice Boltzmann method simulation for CuO–water nanofluid flow in a porous enclosure with hot obstacle. *J Mol Liq.* 2017;243(Supplement C):249–56.
18. Islam MR, Shabani B, Rosengarten G. Nanofluids to improve the performance of PEM fuel cell cooling systems: a theoretical approach. *Appl Energy.* 2016;178(Supplement C):660–71.
19. Colangelo G, Favale E, de Risi A, Laforgia D. A new solution for reduced sedimentation flat panel solar thermal collector using nanofluids. *Appl Energy.* 2013;111(Supplement C):80–93.
20. Mahian O, Kianifar A, Kalogirou SA, Pop I, Wongwises S. A review of the applications of nanofluids in solar energy. *Int J Heat Mass Transf.* 2013;57(2):582–94.
21. Khawaji AD, Kutubkhanah IK, Wie J-M. Advances in seawater desalination technologies. *Desalination.* 2008;221(1):47–69.
22. Thu K, Saha BB, Chakraborty A, Chun WG, Ng KC. Study on an advanced adsorption desalination cycle with evaporator–condenser heat recovery circuit. *Int J Heat Mass Transf.* 2011;54(1–3):43–51.
23. Kabeel AE, Hamed AM, El-Agouz SA. Cost analysis of different solar still configurations. *Energy.* 2010;35(7):2901–8.
24. Hasnain SM, Alajlan SA. Coupling of PV-powered RO brackish water desalination plant with solar stills. *Desalination.* 1998;116(1):57–64.
25. Shatat M, Riffat SB. Water desalination technologies utilizing conventional and renewable energy sources. *Int J Low-Carbon Technol.* 2014;9(1):1–19.
26. Sivakumar V, Sundaram EG. Improvement techniques of solar still efficiency: a review. *Renew Sustain Energy Rev.* 2013;28:246–64.
27. Panchal HN, Patel S. An extensive review on different design and climatic parameters to increase distillate output of solar still. *Renew Sustain Energy Rev.* 2017;69:750–8.

28. Karakilcik M, Kıymaç K, Dincer I. Experimental and theoretical temperature distributions in a solar pond. *Int J Heat Mass Transf*. 2006;49(5):825–35.
29. Otanicar TP, Golden JS. Comparative environmental and economic analysis of conventional and nanofluid solar hot water technologies. *Environ Sci Technol*. 2009;43(15):6082–7.
30. Velmurugan V, Srithar K. Performance analysis of solar stills based on various factors affecting the productivity—a review. *Renew Sustain Energy Rev*. 2011;15(2):1294–304.
31. Tsoutsos T, Frantzeskaki N, Gekas V. Environmental impacts from the solar energy technologies. *Energy Policy*. 2005;33(3):289–96.
32. Duffie JA, Beckman WA. *Solar engineering of thermal processes*. Hoboken: Wiley; 1980.
33. Tiwari GN, Singh HN, Tripathi R. Present status of solar distillation. *Sol Energy*. 2003;75(5):367–73.
34. Sampathkumar K, Arjunan TV, Pitchandi P, Senthilkumar P. Active solar distillation—a detailed review. *Renew Sustain Energy Rev*. 2010;14(6):1503–26.
35. Rajaseenivasan T, Murugavel KK, Elango T, Hansen RS. A review of different methods to enhance the productivity of the multi-effect solar still. *Renew Sustain Energy Rev*. 2013;17:248–59.
36. Foster R, Ghassemi M, Cota A. *Solar energy: renewable energy and the environment*. Boca Raton: CRC Press; 2009.
37. Kabeel A, Omara Z, Essa F, Abdullah A. Solar still with condenser—a detailed review. *Renew Sustain Energy Rev*. 2016;59(C):839–57.
38. Sheikholeslami M, Darzi M, Li Z. Experimental investigation for entropy generation and exergy loss of nano-refrigerant condensation process. *Int J Heat Mass Transf* 2018;125:1087–95.
39. Warriar P, Teja A. Effect of particle size on the thermal conductivity of nanofluids containing metallic nanoparticles. *Nanoscale Res Lett*. 2011;6(1):247.
40. Saidur R, Kazi SN, Hossain MS, Rahman MM, Mohammed HA. A review on the performance of nanoparticles suspended with refrigerants and lubricating oils in refrigeration systems. *Renew Sustain Energy Rev*. 2011;15(1):310–23.
41. Yiamsawas T, Mahian O, Dalkilic AS, Kaewnai S, Wongwises S. Experimental studies on the viscosity of TiO₂ and Al₂O₃ nanoparticles suspended in a mixture of ethylene glycol and water for high temperature applications. *Appl Energy*. 2013;111(Supplement C):40–5.
42. Sheikholeslami M, Darzi M, Sadoughi MK. Heat transfer improvement and pressure drop during condensation of refrigerant-based nanofluid; an experimental procedure. *Internat J Heat Mass Transfer* 2018;122:643–650.
43. Reddy PS, Chamkha AJ. Influence of size, shape, type of nanoparticles, type and temperature of the base fluid on natural convection MHD of nanofluids. *Alex Eng J*. 2016;55(1):331–41.
44. Buongiorno J. Convective transport in nanofluids. *J Heat Transf*. 2005;128(3):240–50.
45. Sahota L, Tiwari GN. Effect of nanofluids on the performance of passive double slope solar still: a comparative study using characteristic curve. *Desalination*. 2016;388(Supplement C):9–21.
46. Samee MA, Mirza UK, Majeed T, Ahmad N. Design and performance of a simple single basin solar still. *Renew Sustain Energy Rev*. 2007;11(3):543–9.
47. Rashidi S, Akar S, Bovand M, Ellahi R. Volume of fluid model to simulate the nanofluid flow and entropy generation in a single slope solar still. *Renew Energy*. 2018;115:400–10.
48. Gnanadason MK, Kumar PS, Jemilda G, Jasper SS. Effect of nanofluids in a modified vacuum single basin solar still. *Int J Sci Eng Res*. 2012;3:2229–518.
49. Ali MT, Fath HES, Armstrong PR. A comprehensive techno-economical review of indirect solar desalination. *Renew Sustain Energy Rev*. 2011;15(8):4187–99.
50. Prakash P, Velmurugan V. Parameters influencing the productivity of solar stills—a review. *Renew Sustain Energy Rev*. 2015;49:585–609.
51. Sain MK, Kumawat G. Performance enhancement of single slope solar still using nano-particles mixed black paint. *Adv Nanosci Technol Int J*. 2015;1:55–65.
52. Kabeel A, Omara Z, Essa F. Numerical investigation of modified solar still using nanofluids and external condenser. *J Taiwan Inst Chem Eng*. 2017;75:77–86.
53. Kabeel AE, Omara ZM, Essa FA. Enhancement of modified solar still integrated with external condenser using nanofluids: an experimental approach. *Energy Convers Manag*. 2014;78(Supplement C):493–8.
54. Manokar AM, Murugavel KK, Esakkimuthu G. Different parameters affecting the rate of evaporation and condensation on passive solar still—a review. *Renew Sustain Energy Rev*. 2014;38:309–22.
55. Kabeel AE, Omara ZM, Essa FA. Improving the performance of solar still by using nanofluids and providing vacuum. *Energy Convers Manag*. 2014;86(Supplement C):268–74.
56. Thakur AK, Agarwal D, Khandelwal P, Dev S. Comparative study and yield productivity of nano-paint and nano-fluid used in a passive-type single basin solar still. In: SenGupta S, Zobaa AF, Sherpa KS, Bhoi AK, editors. *Advances in smart grid and renewable energy: proceedings of ETAEERE-2016*. Singapore: Springer Singapore; 2018. p. 709–16.
57. Muftah AF, Alghoul MA, Fudholi A, Abdul-Majeed MM, Sopian K. Factors affecting basin type solar still productivity: a detailed review. *Renew Sustain Energy Rev*. 2014;32:430–47.
58. Rajasekhar G, Eswaramoorthy M. Performance evaluation on solar still integrated with nano-composite phase change materials. *Appl Solar Energy*. 2015;51(1):15–21.
59. Al-Hayeka I, Badran OO. The effect of using different designs of solar stills on water distillation. *Desalination*. 2004;169(2):121–7.
60. Panchal HN. Use of thermal energy storage materials for enhancement in distillate output of solar still: a review. *Renew Sustain Energy Rev*. 2016;61:86–96.
61. Sahota L, Tiwari GN. Effect of Al₂O₃ and TiO₂–water-based nanofluids on heat transfer coefficients of passive double slope solar still. *Int J Energy Environ Econ*. 2016;24(1):3.
62. Sahota L, Tiwari G. Effect of Al₂O₃ nanoparticles on the performance of passive double slope solar still. *Sol Energy*. 2016;130:260–72.
63. Sahota L, Tiwari G. Energy matrices, enviroeconomic and exergoeconomic analysis of passive double slope solar still with water based nanofluids. *Desalination*. 2017;409:66–79.
64. Sahota L, Tiwari G. Exergoeconomic and enviroeconomic analyses of hybrid double slope solar still loaded with nanofluids. *Energy Convers Manag*. 2017;148:413–30.
65. Sahota L, Tiwari G. Analytical characteristic equation of nanofluid loaded active double slope solar still coupled with helically coiled heat exchanger. *Energy Convers Manag*. 2017;135:308–26.
66. Rashidi S, Bovand M, Rahbar N, Esfahani JA. Steps optimization and productivity enhancement in a nanofluid cascade solar still. *Renew Energy*. 2018;118(Supplement C):536–45.
67. Kaviti AK, Yadav A, Shukla A. Inclined solar still designs: a review. *Renew Sustain Energy Rev*. 2016;54:429–51.
68. Rashidi S, Bovand M, Rahbar N, Esfahani JA. Steps optimization and productivity enhancement in a nanofluid cascade solar still. *Renew Energy*. 2018;118:536–45.

69. Manchanda H, Kumar M. "A comprehensive decade review and analysis on designs and performance parameters of passive solar still. *Renew Wind Water Sol.* 2015;2(1):17.
70. Saleh SM, Soliman AM, Sharaf MA, Kale V, Gadgil B. Influence of solvent in the synthesis of nano-structured ZnO by hydrothermal method and their application in solar-still. *J Environ Chem Eng.* 2017;5(1):1219–26.
71. Arunkumar T, et al. Effect of heat removal on tubular solar desalting system. *Desalination.* 2016;379:24–33.
72. Arunkumar T, Velraj R, Denkenberger DC, Sathyamurthy R, Kumar KV, Ahsan A. Productivity enhancements of compound parabolic concentrator tubular solar stills. *Renew Energy.* 2016;88:391–400.
73. Omara Z, Kabeel A, Essa F. Effect of using nanofluids and providing vacuum on the yield of corrugated wick solar still. *Energy Convers Manag.* 2015;103:965–72.
74. Omara ZM, Kabeel AE, Abdullah AS. A review of solar still performance with reflectors. *Renew Sustain Energy Rev.* 2017;68:638–49.
75. Sharshir SW, et al. Enhancing the solar still performance using nanofluids and glass cover cooling: experimental study. *Appl Therm Eng.* 2017;113(Supplement C):684–93.
76. Sharshir S, et al. Enhancing the solar still performance using nanofluids and glass cover cooling: experimental study. *Appl Therm Eng.* 2017;113:684–93.
77. Gupta B, Shankar P, Sharma R, Baredar P. Performance enhancement using nano particles in modified passive solar still. *Procedia Technol.* 2016;25:1209–16.
78. Kabeel A, Omara Z, Essa F, Abdullah A, Arunkumar T, Sathyamurthy R. Augmentation of a solar still distillate yield via absorber plate coated with black nanoparticles. *Alex Eng J.* 2017;56(4):433–8.
79. Chen W, Zou C, Li X, Li L. Experimental investigation of SiC nanofluids for solar distillation system: stability, optical properties and thermal conductivity with saline water-based fluid. *Int J Heat Mass Transf.* 2017;107:264–70.
80. Rashidi S, Akar S, Bovand M, Ellahi R. Volume of fluid model to simulate the nanofluid flow and entropy generation in a single slope solar still. *Renew Energy.* 2018;115(Supplement C):400–10.
81. Pk N, Sathyamurthy R. Improving the yield of freshwater and exergy analysis of conventional solar still with different nanofluids. *FME Trans.* 2017;45(4):525.
82. Sahota L, Shyam, Tiwari GN. Energy matrices, enviroeconomic and exergoeconomic analysis of passive double slope solar still with water based nanofluids. *Desalination.* 2017;409(Supplement C):66–79.
83. Gamit ID, Modi K. Comparative analysis of double slope solar still using Al_2O_3 nanofluid with conventional double slope solar still. *Int J Adv Res Innov Ideas Educ.* 2016;3(2):2384.
84. Chen W, Zou C, Li X, Li L. Experimental investigation of SiC nanofluids for solar distillation system: stability, optical properties and thermal conductivity with saline water-based fluid. *Int J Heat Mass Transf.* 2017;107(Supplement C):264–70.
85. Gupta B, Shankar P, Sharma R, Baredar P. Performance enhancement using nano particles in modified passive solar still. *Procedia Technol.* 2016;25(Supplement C):1209–16.
86. Sellami MH, Guemari S, Touahir R, Loudiyi K. Solar distillation using a blackened mixture of Portland cement and alluvial sand as a heat storage medium. *Desalination.* 2016;394(Supplement C):155–61.
87. Sharma SJ, Modi K. Techniques to improve productivity of spherical solar still. *Int J Adv Res Innov Ideas Educ.* 2016;2(3):997–1001.
88. Arunkumar T, et al. Effect of heat removal on tubular solar desalting system. *Desalination.* 2016;379(Supplement C):24–33.
89. Yadav S, Sudhakar K. Different domestic designs of solar stills: a review. *Renew Sustain Energy Rev.* 2015;47:718–31.
90. Kabeel A, El-Said EM. Applicability of flashing desalination technique for small scale needs using a novel integrated system coupled with nanofluid-based solar collector. *Desalination.* 2014;333(1):10–22.
91. Elango T, Kannan A, Murugavel KK. Performance study on single basin single slope solar still with different water nanofluids. *Desalination.* 2015;360:45–51.
92. Qin Yinghong, Hiller Jacob E, Meng Demiao. Linearity between pavement thermophysical properties and surface temperatures. *J Mater Civ Eng.* 2019. [https://doi.org/10.1061/\(ASCE\)MT.1943-5533.0002890](https://doi.org/10.1061/(ASCE)MT.1943-5533.0002890).
93. Bellos E, Tzivanidis C. Thermal efficiency enhancement of nanofluid-based parabolic trough collectors. *J Therm Anal Calorim.* 2018. <https://doi.org/10.1007/s10973-018-7056-7>.
94. Sheikholeslami M, Rezaeianjouybari B, Darzi M, Shafee A, Li Z, Nguyen TK. Application of nano-refrigerant for boiling heat transfer enhancement employing an experimental study. *Int J Heat Mass Transf.* 2019;141:974–80.
95. Li Z, Saleem S, Shafee A, Chamkha AJ, Du S. Analytical investigation of nanoparticle migration in a duct considering thermal radiation. *J Therm Anal Calorim.* 2019;135:1629–41.
96. Sheikholeslami M, Jafaryar M, Ali JA, Hamad SM, Divsalar A, Shafee A, Nguyen-Thoi T, Li Z. Simulation of turbulent flow of nanofluid due to existence of new effective turbulator involving entropy generation. *J Mol Liq.* 2019;291:111283.
97. Saleem S, Nadeem S, Rashidi MM, Raju CS. An optimal analysis of radiated nanomaterial flow with viscous dissipation and heat source. *Microsyst Technol.* 2019;25:683–9.
98. Sheikholeslami M, Jafaryar M, Hedayat M, Shafee A, Li Z, Nguyen TK, Bakouri M. Heat transfer and turbulent simulation of nanomaterial due to compound turbulator including irreversibility analysis. *Int J Heat Mass Transf.* 2019;137:1290–300.
99. Kumar RA, Babu BG, Mohanraj M. Thermodynamic performance of forced convection solar air heaters using pin-fin absorber plate packed with latent heat storage materials. *J Therm Anal Calorim.* 2016;126:1657–78.
100. Gao W, Yan L, Shi L. Generalized Zagreb index of polyomino chains and nanotubes. *Optoelectron Adv Mater Rapid Commun.* 2017;11(1–2):119–24.
101. Sadiq MA, Khan AU, Saleem S, Nadeem S. Numerical simulation of oscillatory oblique stagnation point flow of a magneto micropolar nanofluid. *RSC Adv.* 2019;9:4751–64.
102. Sheikholeslami M. New computational approach for exergy and entropy analysis of nanofluid under the impact of Lorentz force through a porous media. *Comput Methods Appl Mech Eng.* 2019;344:319–33.
103. Raju CSK, Saleem S, Mamatha SU, Hussain I. Heat and mass transport phenomena of radiated slender body of three revolutions with saturated porous: Buongiorno's model. *Int J Therm Sci.* 2018;132:309–15.
104. Sheikholeslami M. Numerical approach for MHD Al_2O_3 -water nanofluid transportation inside a permeable medium using innovative computer method. *Comput Methods Appl Mech Eng.* 2019;344:306–18.
105. Sheikholeslami M, Jafaryar M, Shafee A, Li Z. Nanofluid heat transfer and entropy generation through a heat exchanger considering a new turbulator and CuO nanoparticles. *J Therm Anal Calorim.* 2019. <https://doi.org/10.1007/s10973-018-7866-7>.
106. Qin Y, Zhao Y, Chen X, Wang L, Li F, Bao T. Moist curing increases the solar reflectance of concrete. *Constr Build Mater.* 2019;215:114–8.
107. Rashidi S, Javadi P, Esfahani JA. Second law of thermodynamics analysis for nanofluid turbulent flow inside a solar heater

- with the ribbed absorber plate. *J Therm Anal Calorim.* 2018. <https://doi.org/10.1007/s10973-018-7070-9>.
108. Gao W, Wang WF. The eccentric connectivity polynomial of two classes of nanotubes. *Chaos Solitons Fractals.* 2016;89:290–4.
109. Rashidi S, Eskandarian M, Mahian O, Poncet S. Combination of nanofluid and inserts for heat transfer enhancement. *J Therm Anal Calorim.* 2018. <https://doi.org/10.1007/s10973-018-7070-9>.
110. Sheikholeslami M, Sheremet MA, Shafee A, Li Z. CVFEM approach for EHD flow of nanofluid through porous medium within a wavy chamber under the impacts of radiation and moving walls. *J Therm Anal Calorim.* 2019. <https://doi.org/10.1007/s10973-019-08235-3>.
111. Stalin PMJ, Arjunan TV, Matheswaran MM, Sadanandam N. Experimental and theoretical investigation on the effects of lower concentration CeO₂/water nanofluid in flat-plate solar collector. *J Therm Anal Calorim.* 2017. <https://doi.org/10.1007/s10973-017-6865-4>.

Publisher's Note Springer Nature remains neutral with regard to jurisdictional claims in published maps and institutional affiliations.